Mechanical stability of ordered droplet packings in microfluidic channels

Cite as: Appl. Phys. Lett. **99**, 244104 (2011); https://doi.org/10.1063/1.3665185
Submitted: 17 August 2011 . Accepted: 08 November 2011 . Published Online: 16 December 2011

Jean-Baptiste Fleury, Ohle Claussen, Stephan Herminghaus, Martin Brinkmann, and Ralf Seemann

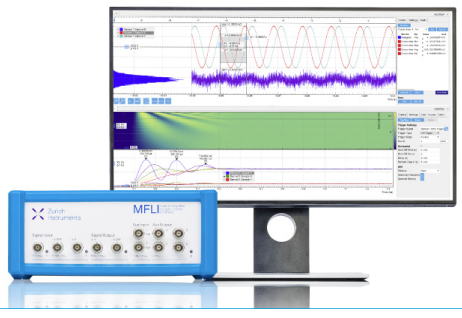

Mechanical stability of ordered droplet packings in microfluidic channels

Jean-Baptiste Fleury,[1] Ohle Claussen,[2] Stephan Herminghaus,[2] Martin Brinkmann,[2] and Ralf Seemann[1,2,a)]
[1]*Experimental Physics, Saarland University, 66123 Saarbrücken, Germany*
[2]*Max Planck Institute for Dynamics and Self-Organization, 37077 Göttingen, Germany*

(Received 17 August 2011; accepted 8 November 2011; published online 16 December 2011; publisher error corrected 27 December 2011)

The mechanical response and stability of one and two-row packing of monodisperse emulsion droplets are studied in quasi 2d microchannels under longitudinal compression. Depending on the choice of parameter, a considered droplet arrangement is either transformed continuously into another packing under longitudinal compression or becomes mechanically unstable and segregates into domains of higher and lower packing fraction. Our experimental results are compared to analytical calculations for 2d-droplet arrangements with good quantitative agreement. This study also predicts important consequences for the stability of droplet arrangements in flowing systems.
 [doi:10.1063/1.3665185]

In most applications of discrete microfluidics, continuous trains of droplets are generated and manipulated as they are flowing through a network of microchannels. Depending on the ratio between the dispersed and the continuous phase, a rich variety of stable droplet packing can be found and topologically reorganized.[1,2] Also, a number of studies has been devoted to explore static and flowing packing of bubbles under various conditions.[3–5] Despite these studies, the range of accessible droplet arrangements under certain pressure or volume conditions is still unknown. To close this gap, we explore the self-organization of static, quasi two-dimensional droplets in flat microchannels in response to an externally applied longitudinal compression. For simplicity, we restrict our study to the three fundamental quasi-two dimensional droplet arrangements in microfluidic channels which are sketched in Fig. 1(a): dilute two-row zigzag, one-row bamboo, and dense two-row staircase structures.[6]

For the experimental study, we developed the microfluidic setup which is sketched in Fig. 1(b) and which allows to produce, stop, trap, and compress monodisperse droplet packings. The microfluidic devices were fabricated in Sylgard 184 (Dow Corning) by standard techniques.[2] Water droplets are produced in a continuous mineral oil phase (Sigma M5904) using a step emulsification device.[7] Constant volumetric flow rates were achieved by custom made computer controlled syringe pumps. To guarantee a stable production of monodisperse droplets and to suppress subsequent droplet coalescence, the non-ionic surfactant Span 80 (Sigma S6760) was added to the continuous phase[10] with a concentration of 1.5% by weight lowering the oil/water interfacial energy to $\gamma = 3.7\,\mathrm{mN/m}$ at 30 °C. The horizontal channel in Fig. 1(b) has a width of $W = 210\,\mu\mathrm{m}$ and a height of $H = 30\,\mu\mathrm{m}$ and the droplets confined in this channel may be approximate as quasi-two dimensional discs of an incompressible fluid. Accordingly, the area fraction covered by the droplet packing relative to the channel area, φ, is a good estimate of the actual volume fraction and can be easily derived from optical micrographs. Before each measurement, the horizontal channel in Fig. 1(b) is filled with monodisperse droplets. The liquid flow in the device is stopped and two liquid plugs of fluorinated oil (FC40, ABCR, Germany) were introduced from the two inlets 1 and 2 using syringe pumps. As the fluorinated oil is immiscible with the two other liquids, i.e., water and mineral oil, the liquid plugs act like movable pistons and allow to confine several tens of droplets in the horizontal channel between the inlets 1 and 2. In a next step, one of the two FC40 plugs is disconnected from the pump and connected to a hydrostatic FC40 reservoir by a two-way valve. The hydrostatic pressure $P_h = \rho g h$ in the plug can be precisely adjusted by the reservoir height h (density of FC40, $\rho = 1855\,\mathrm{kg/m^3}$). The resulting compressive force F_c applied to the droplet packing can be calculated from the hydrostatic pressure and the cross sectional area of the channel, $F_c = P_h WH$. The reservoir height h is measured relative to the height where the plug just invades the channel and does not yet touch the droplets. The channel section where the droplets are confined is connected to a reservoir of

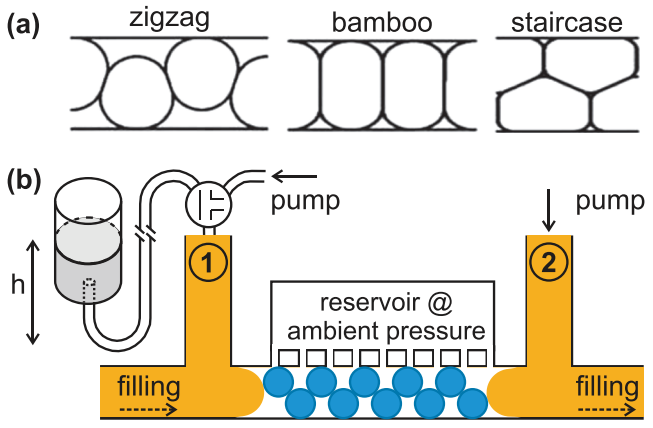

FIG. 1. (Color online) (a) Three fundamental packing geometries consisting of congruent droplets: two-row zigzag structure, one-row bamboo structure, and two-row staircase structure. (b) Sketch of the central part of the microfluidic device.

a)Author to whom correspondence should be addressed. Electronic mail: r.seemann@physik.uni-saarland.de.

constant ambient pressure via several small side channels which facilitate the exchange of the continuous phase but do not allow the droplets to pass. Thus, the applied force F_c does not act on the continuous phase but compresses the droplet packing which responds like an elastic spring. In mechanical equilibrium, the applied force F_c is balanced by the elastic force, F_e, in the droplet packing which can be calculated analytically. The preparation of a dilute zigzag arrangement as starting condition is finalized by closing outlet 2 and giving the system sufficient time to mechanically equilibrate. The force F_c on the droplet packing is gradually increased, or decreased, by varying the reservoir height in small steps. Typically, steps of 50 μm were applied resulting in force variations of 5.7 nN. Between subsequent steps, the system is given sufficient time ($\geq$5 min) to exchange continuous phase with the reservoir and to reach isobaric conditions in the droplet packing. Images of compression cycles are shown in Fig. 2 for two different droplet confinements.[9] The dimensionless droplet confinement is defined in 2d as the area of a single droplet A, divided by the squared channel width, A/W^2.

During a compression-decompression cycle, we optically measure the area fraction φ as function of the applied force F_c for several droplet confinements, A/W^2; c.f. Fig. 3. Depending on the droplet confinement, two different scenarios of structural transitions are observed: For large droplet confinements, $A/W^2 \gtrsim 0.525 \pm 0.01$, the droplet arrangements evolve continuously from a loose zigzag packing into a dense bamboo packing upon compression, c.f. Fig. 2(a) and symbols in Fig. 3(a). In this case, the droplet rearrangement is fully reversible during a compression-decompression cycle.

For small confinements, $A/W^2 \lesssim 0.46 \pm 0.01$, the droplet arrangements evolve between a dilute zigzag packing and a dense staircase structure. Here, a discontinuous and hysteretic transition is observed where the area fraction φ "jumps" at constant applied force F_c between two limiting values of φ. During the transient compression, a dilute zigzag packing and a dense staircase packing can be observed while the staircase structure grows on cost of the zigzag structure, c.f. Fig. 2(b) and symbols in Fig. 3(b). Vice versa, the zigzag structure grows on cost of the staircase structure during the transient decompression at reduced F_c compared to the compression cycle. Droplet rearrangements at intermediate confinements between the above defined two scenarios, i.e., in the range $0.46 \lesssim A/W^2 \lesssim 0.525$, can hardly be accessed experimentally as the resulting droplet packing are very sensitive to the presence of the small side channels.

To understand the experimentally found behavior in more detail, we also studied the mechanical properties of quasi 2d droplet arrangements analytically. The droplet

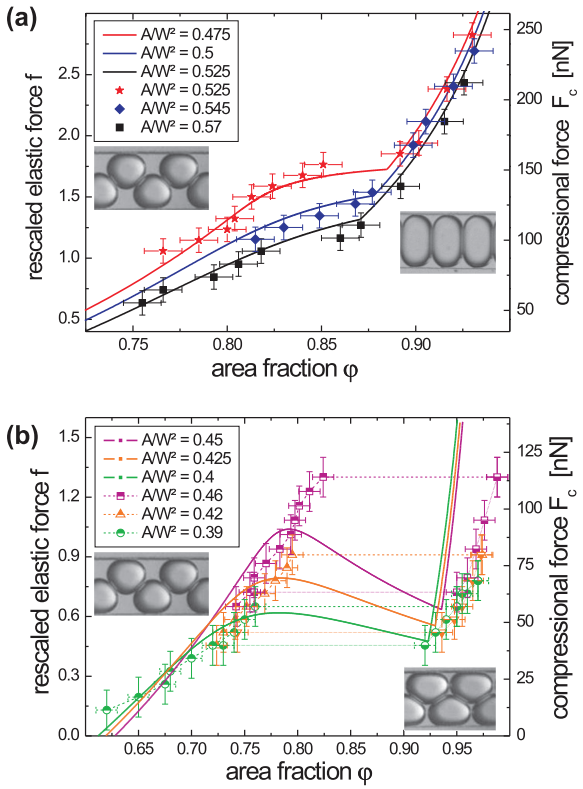

FIG. 3. (Color online) Experimentally, applied compression force F_c, respectively, analytically calculated rescaled elastic force $f = F_e \cdot 4/\pi\gamma H$ as function of the self-adjusting area fraction φ of 2d droplet packing for several confinement values. (a) For large confinement ($A/W^2 \gtrsim 0.525$ exp. and $\geq$ 0.471 theo.) reversible transitions during a compression-decompression cycle are found. (b) For small confinement ($A/W^2 \lesssim 0.46$ exp. and <0.471 theo.) hysteretic transitions are observed. Top and bottom half filled symbols correspond to a compression and decompression cycle, respectively.

shapes in mechanical equilibrium are constructed according to the following rules: Owing to the Laplace law, the mean curvature of the droplet interface has to be identical in every point in contact with the continuous phase. Since the out of plane curvature of the droplet interface is always $2/H$ in the leading order, the in-plane curvature of the droplet boundary with the continuous phase has to be identical. Because of congruency, the Laplace pressure is the same in all droplets implying straight boundaries between two touching droplets. Based on these rules, we analytically constructed the three relevant droplet packing and determined the perimeter ℓ_d of the droplet contour, the area A enclosed by it, and the corresponding area fraction φ.[6] This allowed us to compute the interfacial energy $E_d = \tau\ \ell_d$ of the droplets as a function of droplet area and packing fraction, where $\tau = \pi\gamma H/4$ is the

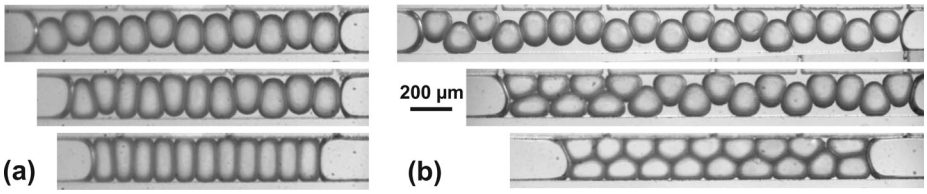

FIG. 2. Optical micrographs showing structural transitions upon longitudinal compression. (a) For droplets at large confinement, $A/W^2 = 0.525$, a zigzag structure transforms into a bamboo packing ($\Delta F_c = 146$ nN between top and bottom image). (b) For small confinement, $A/W^2 = 0.42$, a zigzag structure transforms into a staircase packing ($\Delta F_c = 82.8$ nN).[9] (enhanced online) [URL: http://dx.doi.org/10.1063/1.3665185.1]

effective line tension of the two dimensional droplet contour in a flat Hele-Shaw geometry.[6,8]

The elastic force F_e of the droplet packing can be obtained as the derivative of the interfacial energy $E = NE_d$ of a train of N droplets with respect to the length L of the droplet train for fixed A

$$F_e = -\left.\frac{\partial E}{\partial L}\right|_A = \left.\frac{\varphi^2}{A}\frac{\partial E_d}{\partial \varphi}\right|_A. \quad (1)$$

Based on the results of the theoretical considerations in Ref. 6, we analytically computed the dimensionless elastic force $f = F_e/\tau$ from the interfacial energy of the considered droplet packing as function of the droplet confinement A/W^2 and the area fraction φ. The calculated elastic force $f(\varphi)$ is plotted as solid lines in Fig. 3 for several droplet confinement.

In the following, the analytical results will be discussed in comparison with the experimental results: Generally, a droplet arrangement is mechanically stable against rearrangements if the force into longitudinal direction increases upon compression, $\partial f/\partial\varphi \geq 0$. Inspection of Fig. 3(a) reveals that this condition is fulfilled for large confinements over the entire range of area fractions resulting in continuous and reversible transitions between dilute zigzag and dense bamboo structures. The condition for large confinement was determined to $A/W^2 \gtrsim 0.49$ experimentally and $A/W^2 \geq 0.471$ analytically. The transition between zigzag and bamboo packing is related to a kink in the curve, c.f. Fig. 3(a), which moves towards smaller values of the compressive force f and area fraction φ for increasing droplet confinement.

For small confinements, $A/W^2 < 0.49$ as determined experimentally and $A/W^2 < 0.471$ analytically, we encounter both, mechanically stable and unstable droplet arrangements. The negative compressibility, $\partial f/\partial\varphi \leq 0$, of the unstable droplet arrangements leads to discontinuous transitions between zigzag and staircase structures. For a confinement of e.g. $A/W^2 = 0.39$, as shown by the circles in Fig. 3(b), the negative compressibility applies for $0.75 \lesssim \varphi \lesssim 0.925$. To understand the discontinuous transition for small confinement, let us follow the calculated solid curve for the confinement of $A/W^2 = 0.39$ starting at low area fraction of $\varphi = 0.6$ at a zigzag packing. The dimensionless force f, respectively area fraction, continuously increases upon compression until a local maximum is reached at $\varphi \approx 0.77$. Up to this point, all the droplets can be found in the same stable zigzag arrangement as $\partial f/\partial\varphi \geq 0$. Further increase of f results in a transient separation of the droplet packing in two fractions, one with higher and another with lower area fraction φ, i.e., a dense staircase and a dilute zigzag arrangement, see also the middle image of Fig. 2(b). Since the compressive force becomes smaller beyond the local maximum, this transformation has to continue until all droplets arrange in a dense staircase structure. In this transient regime, where $\partial f/\partial\varphi \leq 0$, the experimental data will not follow the calculated (solid) curve but will "jump" along the dashed horizontal line at constant compressional stress of $f \approx 0.6$ from the local maximum at $\varphi \approx 0.77$ to $\varphi \approx 0.96$ where $\partial f/\partial\varphi \geq 0$, again. Thus for further increase of the lateral force, the experimental data follow again the trend of the calculated line. Similarly upon decompression, the dense staircase arrangement will irreversibly expand into a dilute zigzag structure at constant lateral compression of $f \approx 0.45$ once the force reaches a local minimum at $\varphi \approx 0.92$ where the theoretical curve starts to have a negative slope, $\partial f/\partial\varphi \leq 0$. Thus, the force difference between the local maximum and the local minimum of the calculated curve determines the opening of the experimentally found hysteresis loop. For both large and small confinement, the agreement between analytical and experimental data is good within the experimental error. Systematic deviations are only observed for very large volume fractions, $\varphi \geq 0.92$, c.f. Fig. 3(b), where the theoretical curves have a steeper slope than the experimental data. The systematic deviation is most probably caused by the fact that the assumption of an effectively 2d experimental system is not fulfilled any more and the curvature in the direction perpendicular to the considered plane is also affected by the compression.

For the simplest and most fundamental 2d one- and two-row droplet arrangements and their transitions, a strong impact of droplet confinement was found upon variations in the applied lateral compression force. In particular, we found a discontinuous transition between zigzag and staircase packing at low droplet confinement which is linked to bi-stability and hysteresis of the packing geometry. But even though exclusively static droplet arrangements were considered, this finding is expected to be of fundamental importance for flowing systems as it shall not be possible to generate mechanically stable droplet trains at confinements $A/W^2 < 0.471$ for all packing fractions, i.e. having a negative compressibility $\partial f/\partial\varphi \leq 0$. This is particularly relevant as the regime of volume fractions and droplet confinement linked to bi-stability is rather large: $0.782 \lesssim \varphi \lesssim 1.0$ for $0.28 \leq A/W^2 \leq 0.47$.

Funding was provided by the Deutsche Forschungsgemeinschaft Grant Nos. SE 1118/4 and BR 3749/1. Further, we acknowledge support from the BP International - 'ExploRe' program.

[1]S. Hutzler, N. Peron, D. Weaire, and W. Drenckhan, Eur. Phys. J. E **14**, 381 (2004).
[2]E. Surenjav, S. Herminghaus, C. Priest, and R. Seemann, Lab Chip **9**, 325 (2009).
[3]P. Garstecki and G. M. Whitesides, Phys. Rev. E **73**, 031603 (2006).
[4]J.-P. Raven and P. Marmottant, Phys. Rev. Lett. **102**, 084501 (2009).
[5]W. Drenckhan, S. J. Cox, G. Delaney, H. Holste, and D. Weaire, Colloids Surf., A **263**, 52 (2005).
[6]J. O. Claussen, S. Herminghaus, and M. Brinkmann, "Packings of monodisperse emulsions in flat microfluidic channels," Phys. Rev. E. (submitted).
[7]V. Chokkalingan, S. Herminghaus, and R. Seemann, Appl. Phys. Lett. **93**, 254101 (2008).
[8]C.-W. Park and G. M. Homsy, J. Fluid Mech. **139**, 291 (1984).
[9]See supplementary material at http://dx.doi.org/10.1063/1.3665185 for supporting movies which show the compression of a zigzag droplet arrangement to a bamboo arrangement at large droplet confinement $A/W^2 > 0.471$ and the compression of a zigzag droplet arrangement to a staircase arrangement at small droplet confinement $A/W^2 < 0.471$, for a stepwise increase of the applied force F_c.
[10]To exclude a possible influence of Osmotic pressure, test measurements were performed where the surfactant was dissolved in equal concentrations in both the aqueous and the oily phase. No noticeable difference to the reported results was observed.